Channel-Feedback-Free Transmission for Downlink FD-RAN: A Radio Map Based Complex-Valued Precoding Network Approach

Zhao Jiwei[1,2], Chen Jiacheng[3], Sun Zeyu[1], Shi Yuhang[1], Zhou Haibo[1,*], Xuemin (Sherman) Shen[4]

[1] School of Electronic Science and Engineering, Nanjing University, Nanjing 210023, China
[2] College of Information Science and Electronic Engineering, Zhejiang University, Hangzhou 310058, China
[3] Department of Mathematics and Theories, Peng Cheng Laboratory, Shenzhen 518000, China
[4] Department of Electrical and Computer Engineering, University of Waterloo, Waterloo, Ontario, N2L 3G1, Canada
[*] The corresponding author, email: haibozhou@nju.edu.cn

Cite as: J. Zhao, J. Chen, *et al*., "Channel-feedback-free transmission for downlink fd-ran: A radio map based complex-valued precoding network approach," *China Communications*, 2024, vol. 21, no. 4, pp. 10-22. **DOI**: 10.23919/JCC.fa.2023-0393.202404

Abstract: As the demand for high-quality services proliferates, an innovative network architecture, the fully-decoupled RAN (FD-RAN), has emerged for more flexible spectrum resource utilization and lower network costs. However, with the decoupling of uplink base stations and downlink base stations in FD-RAN, the traditional transmission mechanism, which relies on real-time channel feedback, is not suitable as the receiver is not able to feedback accurate and timely channel state information to the transmitter. This paper proposes a novel transmission scheme without relying on physical layer channel feedback. Specifically, we design a radio map based complex-valued precoding network (RMCPNet) model, which outputs the base station precoding based on user location. RMCPNet comprises multiple subnets, with each subnet responsible for extracting unique modal features from diverse input modalities. Furthermore, the multimodal embeddings derived from these distinct subnets are integrated within the information fusion layer, culminating in a unified representation. We also develop a specific RMCPNet training algorithm that employs the negative spectral efficiency as the loss function. We evaluate the performance of the proposed scheme on the public DeepMIMO dataset and show that RMCPNet can achieve 16% and 76% performance improvements over the conventional real-valued neural network and statistical codebook approach, respectively.

Keywords: beamforming; complex neural networks; deep learning; FD-RAN

Received: Jun. 26, 2023
Revised: Sep. 09, 2023
Editor: Gao Feifei

I. INTRODUCTION

With the explosive growth of mobile communication demand, multi-antenna systems have been widely deployed to provide spectrum-efficient transmission and meet more stringent service requirements [1–7]. Currently, the multi-antenna transmission in 5G is based on codebook and requires feedback to let the transmitter know the channel information in order to precode original signals loaded into different antennas [8]. However, as the number of antennas increases, more pilots are needed to obtain the channel between users and base stations, and the feedback of the channel has become a significant obstacle to achieving higher spectral efficiency of wireless communication [9–12]. Furthermore, considering the channel variation in the practical environment, the feedback information used by base stations for precoding may become outdated

and thus invalid [13, 14]. This leads to a significant decline in the performance of the multi-antenna transmission, especially when the channel changes fast, such as in mobile scenarios. Moreover, in fully decoupled radio access networks (FD-RAN), where the uplink base stations (UBSs) and downlink base stations (DBSs) are physically decoupled, the transmission resources for feedback will be more scarce because users in a wide area share the same control base station [15]. Hence, exploring a new transmission mechanism for massive MIMO becomes an indispensable yet challenging task.

Many recent works have attempted to solve the challenges faced by real-time feedback based communications. With the development of autoencoder, channel state information (CSI) compression based on deep learning has attracted wide attention from researchers [9, 16, 17]. Specifically, CSI is compressed from different frequency domain and spatial domain into bit streams to reduce the amount of feedback data [18–21]. Literature [18] proposes a fully convolutional neural network that incorporates quantization and entropy coding blocks into its design, improving CSI recovery accuracy. Yin *et al.* propose a CSI compression and feedback network based on a self-information model [19]. Literature [20] proposes a network with self-attention and dense refine mechanisms. These neural network-based methods for CSI compression improve feedback accuracy and are suitable for different channel compression ratios. However, these works are still based on real-time feedback of channels. They cannot solve the challenge of outdated channel feedback caused by delay and channel variations.

Another effective approach to deal with outdated channel feedback is to use statistical information of channels for transmission [22–29]. Literature [22] considers the closed-form upper bound of channel capacity when only statistical channel state information is available at the transmitter. [23] derives a closed-form expression for optimal linear precoding. [25] proposes a downlink transmission method based on channel statistical information that considers physical layer security. Muhammad *et al.* design a learning framework that is an integration of a convolutional neural network and a long short term with memory network [29].

Shi *et al.* exploit the structural characteristics for the optimal precoding and propose a deep neural network (DNN) based robust precoding method that learns directly from CSI statistical knowledge [26]. The online computational complexity of the precoder is substantially reduced compared with the existing iterative algorithm while maintaining nearly the same performance.

Location-based precoding techniques have attracted considerable interest from academia owing to the relatively stable statistical characteristics of the channel at the user's location [30–36]. By integrating the navigation information and wireless channel information, Wang et al. enhance the performance of cellular-enabled UAV communications by predicting the angle of arrival [33]. In literature [36], a historical channels based convolutional long short-term memory network is proposed for predicting beamforming. In addition, literature [30, 34] exploits deep learning models to predict the beamforming vectors and further support highly mobile users. Most deep learning based communication techniques are based on real-valued neural networks (RVNN), which may lead to performance degradation for ignoring the correlation between In-Phase/Quardrature (IQ) components [37].

In recent years, complex-valued neural networks (CVNN) [37–39] have been applied to different communication scenarios due to their superior performance and ability to directly process complex-valued data, including channel prediction [40], modulation classification [41], OFDM receiver [42], etc. Literature [42, 43] validate that a deep complex-valued neural network has advantages on complex baseband signal processing. A lightweight CLNet with a complex-valued input layer effectively extracts complex-valued features of input [44]. Nevertheless, to the best of our knowledge, CVNN has not been employed for predicting the precoding for multi-antenna transmission.

The precoding vector/matrix is complex-valued, and the channel statistics are also typically complex. Considering the advantages of complex neural networks in handling complex data, as well as the current dilemma of channel feedback for massive MIMO in 5G [9, 43], we propose a radio map based complex-valued precoding network (RMCPNet) model, which predicts the precoding for transmitting to the user with multiple antennas based on user positions and corresponding complex channel statistics. The contributions of this paper are summarized as follows:

- We propose a downlink channel-feedback-free

transmission approach in the FD-RAN based on user positions and historical channel statistics in the specified spatial domain. The new transmission approach will largely reduce the usage of precious spectrum resources required for channel estimation and feedback.

- Considering that wireless signal processing is usually realized in the complex domain, we propose a complex-valued precoding network based on the radio map. The network can achieve fusion perception of multi-modal information, including user position, transmission/reception correlation matrix, etc., thus improving achievable spectral efficiency.
- Based on publicly available ray tracing data [45], we conduct extensive performance evaluation and provide result analysis for the proposed method. Simulation results show that our proposed method can outperform real-valued neural networks and the statistical codebook scheme.

The rest of the paper is organized as follows. Section II presents the system model and problem formulation. Then, we elaborate on the proposed RMCPNet architecture and corresponding training algorithm in Section II. In Section IV, the simulation scenarios, settings, as well as corresponding simulation results are explained in detail. Finally, we conclude the paper and point out some potential research directions in Section V.

II. SYSTEM MODEL AND PROBLEM FORMULATION

Figure 1 illustrates the downlink transmission in FD-RAN without real-time physical layer feedback. We assume that the edge cloud has stored the spatial domain statistical information about the channel, which is periodically updated to adapt to changes in the environment. The edge cloud deploys RMCPNet for user downlink precoding. In this paper, we focus on the single-user case of multi-antenna transmission. First, a user will upload position information to the edge cloud via the control base station. Note that the position feedback is less sensitive than the channel feedback. Then, the edge cloud inputs the user's position information and corresponding channel statistical information stored on the cloud server into RMCPNet to generate precoding and deliver to the serving data base station. Last, the DBS will perform beamforming to serve the user.

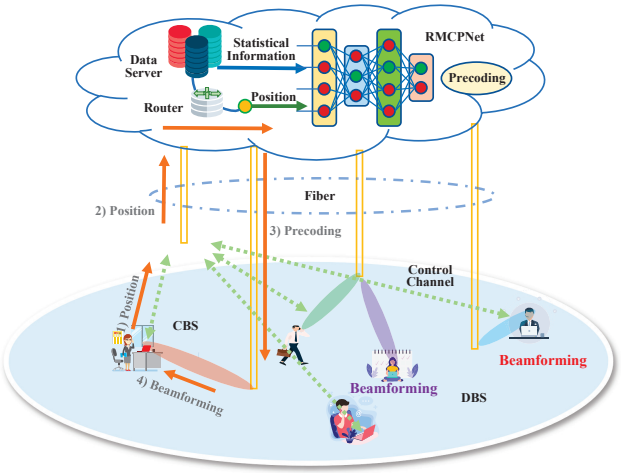

Figure 1. *The proposed channel-feedback-free transmission in the downlink FD-RAN.*

According to [45] the channel between base station b and user k on carrier u is expressed by:

$$\mathbf{h}_k^{b,u} = \sum_{\ell=1}^{L} \sqrt{\frac{\rho_\ell}{U}} e^{j\left(\vartheta_\ell^{b,k} + \frac{2\pi u}{U}\tau_\ell^{b,k} B\right)} \mathbf{a}\left(\phi_{\text{az}}^{b,k}, \phi_{\text{el}}^{b,k}\right), \tag{1}$$

where $\mathbf{a}\left(\phi_{\text{az}}^{b,u}, \phi_{\text{el}}^{b,u}\right)$ is the array response vector of the BS. Since we only consider a single base station serving a single user within a subband, for simplicity of analysis, we denote the channel of user k with

$$\mathbf{H}_k = \mathbf{U}_k \mathbf{G}_k \mathbf{V}_k^H \in \mathbb{C}^{N_k \times M}, \tag{2}$$

where $\mathbf{G}_k \in \mathbb{C}^{N_k \times M}$ represents the beam domain channel matrix, N_k is the number of antennas for user k, and M denotes the number of antennas for DBS. As shown in Eq. (2), $\mathbf{V}$ is independent of the user's position and only depends on the geometry of the base station antenna array. When the base station employs a uniform linear array (ULA) with half-wavelength antenna spacing, we have $\mathbf{H}_k \overset{M\to\infty}{=} \mathbf{U}_k \mathbf{G}_k \mathbf{V}^H$. In this case, $\mathbf{V}$ can be approximated by a discrete Fourier transform (DFT) matrix. We assume that the signal transmitted by user k is $\mathbf{q}_k \in R^M$, which satisfies

$$\mathbb{E}\left\{\mathbf{q}_k \mathbf{q}_{k'}^H\right\} = \begin{cases} 0 & (k' \neq k) \\ 1 & \text{others.} \end{cases} \tag{3}$$

For convenience of notation and to simplify the analysis, we will omit the subscript for user k in the remainder. We assume that the precoding vector for user k at the base station is $\mathbf{w}$, and the signal sent by the base station is

$$\mathbf{x} = \mathbf{w}\mathbf{q}. \tag{4}$$

We assume that $\rho = P_{\max}/\left(M\sigma_n^2\right)$ represents the average signal-to-noise ratio of the user's transmission, where $P_{\max}$ is the maximum power. And, we denote the transmission covariance matrix as $\mathbf{Q} = \mathbb{E}\left\{\mathbf{x}\mathbf{x}_k^H\right\} \in \mathbb{C}^{M\times M}$. Then, the signal received by the user is

$$\mathbf{y} = \mathbf{H}\mathbf{x} + \mathbf{n} \in \mathbb{C}^{N\times 1}, \tag{5}$$

where $\mathbf{n}$ represents the circularly symmetric complex Gaussian noise with zero mean and covariance σ_n^2, i.e., $\mathbf{n} \sim \mathcal{N}_{\mathbb{C}}\left(0, \sigma^2\mathbf{I}_N\right)$.

Based on the channel capacity of MIMO channels, we can obtain the ergodic rate:

$$\begin{aligned} R &= \mathbb{E}\left\{\log\det\left(\mathbf{I} + \rho\mathbf{H}\mathbf{Q}\mathbf{H}^H\right)\right\} \\ &= \mathbb{E}\left\{\log\det\left(\mathbf{I} + \rho\mathbf{U}\mathbf{H}\mathbf{Q}\mathbf{H}^H\mathbf{U}^H\right)\right\} \\ &= \mathbb{E}\left\{\log\det\left(\mathbf{I} + \rho\mathbf{G}\mathbf{V}^H\mathbf{Q}\mathbf{V}\mathbf{G}^H\right)\right\}. \end{aligned} \tag{6}$$

Our problem is to design a precoding strategy for massive MIMO downlink transmission that maximizes spectral efficiency

$$\begin{aligned} \mathcal{F}_1: \max_{\mathbf{Q}} \quad & \mathbb{E}\left\{\log\det\left(\mathbf{I} + \rho\mathbf{G}\mathbf{V}^H\mathbf{Q}\mathbf{V}\mathbf{G}^H\right)\right\} \\ \text{s.t.} \quad & \operatorname{tr}\left(\mathbf{Q}\right) = 1, \mathbf{Q} \succeq 0. \end{aligned} \tag{7}$$

According to [22], the optimal precoding satisfies

$$\mathbf{Q}^{\text{opt}} = \mathbf{V}\mathbf{\Lambda}\mathbf{V}^H. \tag{8}$$

It implies that the downlink transmission signal should be oriented along the base station-related matrix's eigenvectors to achieve the system's maximum spectral efficiency. Hence, beam domain transmission facilitates spectral efficiency optimization in downlink massive MIMO. Consequently, problem $\mathcal{F}_1$ can be reformulated as $\mathcal{F}_2$

$$\begin{aligned} \mathcal{F}_2: \max_{\mathbf{\Lambda}} \quad & \mathbb{E}\left\{\log\det\left(\mathbf{I} + \rho\mathbf{G}\mathbf{\Lambda}\mathbf{G}^H\right)\right\} \\ \text{s.t.} \quad & \operatorname{tr}\left(\mathbf{\Lambda}\right) = 1, \lambda \succeq 0. \end{aligned} \tag{9}$$

For $\mathcal{F}_2$, it is challenging to use the Monte Carlo method to solve. Based on the property of the det matrix, we obtain the following equation:

$$\det\left(\mathbf{I} + \mathbf{A}\mathbf{B}\right) = \det\left(\mathbf{I} + \mathbf{B}\mathbf{A}\right). \tag{10}$$

Applying Jensen's inequality, we can acquire the following:

$$\begin{aligned} C(\boldsymbol{\lambda}) \le C_u(\boldsymbol{\lambda}) &= \log\det\left(\mathbf{I}_{N_r} + \rho\mathbb{E}\left\{\mathbf{G}\mathbf{\Lambda}\mathbf{G}^H\right\}\right) \\ &= \log\det\left(\mathbf{I}_{N_r} + \rho\mathbf{\Lambda}\mathbb{E}\left\{\mathbf{G}^H\mathbf{G}\right\}\right). \end{aligned} \tag{11}$$

Therefore, $\mathcal{F}_2$ can be converted into

$$\begin{aligned} \mathcal{F}_3: \max_{\Lambda} \quad & \log\det\left(\mathbf{I} + \rho\mathbf{\Lambda}\mathbb{E}\left\{\mathbf{G}^{\mathrm{H}}\mathbf{G}\right\}\right) \\ \text{s.t.} \quad & \sum_{i=1}^{M}\lambda_i = 1 \\ & \lambda_i > 0, \forall i = 1, ..., M, \end{aligned} \tag{12}$$

where λ_i is power, and $\mathbb{E}\left\{\mathbf{G}^{\mathrm{H}}\mathbf{G}\right\}$ is the statistical information of the channel. Hence, the base station's precoding can be derived from the channel's statistical information.

III. RADIO MAP BASED CHANNEL-FEEDBACK-FREE TRANSMISSION

In the following, we will further derive how to achieve feedback-free transmission.

3.1 Radio Map

From $\mathcal{F}_3$, we can acquire that the precoding $\mathbf{w}$ can be derived from the statistical information of the channel $\mathbb{E}\left\{\mathbf{G}^{\mathrm{H}}\mathbf{G}\right\}$. Given that $\mathbf{H} = \mathbf{U}\mathbf{G}\mathbf{V}^{\mathrm{H}}$, we define the statistical information of the channel as $\mathcal{R}_t$:

$$\begin{aligned} \mathcal{R}_t &\triangleq \mathbb{E}\left\{\mathbf{H}^{\mathrm{H}}\mathbf{H}\right\} \\ &\xlongequal{\mathbf{H}=\mathbf{U}\mathbf{G}\mathbf{V}^{\mathrm{H}}} \mathbb{E}\left\{\left(\mathbf{U}\mathbf{G}\mathbf{V}^{\mathrm{H}}\right)^{\mathrm{H}}\left(\mathbf{U}\mathbf{G}\mathbf{V}^{\mathrm{H}}\right)\right\} \\ &= \mathbb{E}\left\{\mathbf{G}^{\mathrm{H}}\mathbf{G}\right\} \in \mathbb{R}^{M\times M}. \end{aligned} \tag{13}$$

We can analogously define the statistical information $\mathcal{R}_r$:

$$\mathcal{R}_r \triangleq \mathbb{E}\left\{\mathbf{H}\mathbf{H}^{\mathrm{H}}\right\} \in \mathbb{R}^{N\times N}. \tag{14}$$

Based on reference [22], we define the statistical power information

$$\mathcal{R}_p(p) \triangleq \mathbb{E}\left\{\mathbf{H} \odot \mathbf{H}^*\right\} \in \mathbb{R}^{N \times M}, \tag{15}$$

that characterizes the channel.

3.1.1 The Concept of Radio Map

We divide the area of interest $\mathcal{P}$ into different small regions $p \in \mathcal{P}$. In this paper, we refer to map information as $\mathcal{S}$, and the statistical information is denoted as

$$\mathcal{S} \triangleq \left\{\mathbb{E}\left\{\mathbf{H}^{\mathrm{H}}\mathbf{H}\right\}, \mathbb{E}\left\{\mathbf{H}\mathbf{H}^{\mathrm{H}}\right\}, \mathbb{E}\left\{\mathbf{H} \odot \mathbf{H}^*\right\}\right\}, \tag{16}$$

which can completely capture the channel's fading and correlation information. In the following, the radio map is defined as the mapping from each spatial region p to the corresponding channel statistical information

$$\mathcal{S}(p) = \left\{\mathcal{R}_t(p), \mathcal{R}_r(p), \mathcal{R}_p(p)\right\}, \forall p \in \mathcal{P}. \tag{17}$$

3.1.2 The Construction of Radio Map

According to the definition of radio map (17), we assumed that each user would collect channel statistics for their position. After long-term channel statistics, the user will periodically upload the position p and corresponding statistical information $\mathcal{S}(p)$ to the edge cloud. Through broad statistics for all users located at the spatial domain $\mathcal{P}$, the edge cloud will possess complete radio maps for the area, i.e., $\mathcal{S}(p), p \in \mathcal{P}$. During the service period, each user uploads the position p, and the edge cloud determines the precoding vector w based on $\{\mathcal{R}_t(p), \mathcal{R}_r(p), \mathcal{R}_p(p)\}$.

3.2 Radio Map Based Downlink Transmission

In the following, we define the function $\mathbf{w} = f(p, \mathcal{S}(\mathbf{p}))$ as the mapping from the channel statistical information to the corresponding precoding, and our aim is to find such a function. In this paper, we will reformulate our objective as to how to leverage the channel's statistical information $\mathcal{S}(p)$ to obtain the user's precoding

$$\begin{aligned}\mathcal{F}_4 : \arg\max_{f} \quad & \mathbb{E}\Big\{ \log_2 \det\left(\mathrm{I} + \right. \\ & \left. \rho \mathbf{H} f(p, \mathcal{S}(p)) f(p, \mathcal{S}(p))^{\mathrm{H}} \mathbf{H}^{\mathrm{H}}\right) \Big\}.\end{aligned} \tag{18}$$

The function f cannot be derived by theoretical calculation. According to reference [36], such a function f_θ can always be approximated by a neural network when the depth and width of the network reach a certain level. Therefore, in this paper, we adopt a data-driven approach to solve the precoding problem. Assuming that θ is the network parameter, then we have

$$\mathbf{w}_\theta(p) = f_\theta(p, \mathcal{S}(p)), \tag{19}$$

which represents the precoding unit vector when the user is at position p.

Consequently, our ultimate goal is to obtain an optimal model parameter θ that maximizes the user's throughput:

$$\begin{aligned}\mathcal{F}_5 : \arg\max_{\theta} \mathbb{E}\Big\{ & \log_2 \det\left(\mathrm{I} + \right. \\ & \left. \rho \mathbf{H} \mathbf{w}_\theta(p) \mathbf{w}_\theta(p)^{\mathrm{H}} \mathbf{H}^{\mathrm{H}}\right) \Big\},\end{aligned} \tag{20}$$

where ρ denotes the SINR at the receiver. The model parameter θ ultimately determines the network performance.

3.3 Complex Neural Networks

In complex-domain signal processing, the convolution of signals in the time domain is precisely equivalent to the multiplication of signals in the complex domain. As both the precoding and the channel of wireless communication are complex, the complex-domain operation is more appropriate for signal processing, as it can better capture the relationship between the real and imaginary components of the channel.

3.3.1 Complex Layer

For a complex operation f, a complex-valued neuron performs the following processing on a complex input

[37]

$$(f_R(z_I) + f_I(z_R)) + i \cdot (f_R(z_R) - f_I(z_I)), \quad (21)$$

where ψ_R and ψ_I indicate the neuron's real and imaginary processing channels, respectively. For instance, the complex convolution operation is realized as illustrated in Figure 2, where M_I and M_R denote the imaginary and real feature maps, and K_I and K_R denote the imaginary and real convolution kernels [37]. $M_I K_I$ signifies the real-valued convolution outcome between the imaginary convolution kernel K_I and the imaginary feature map M_I.

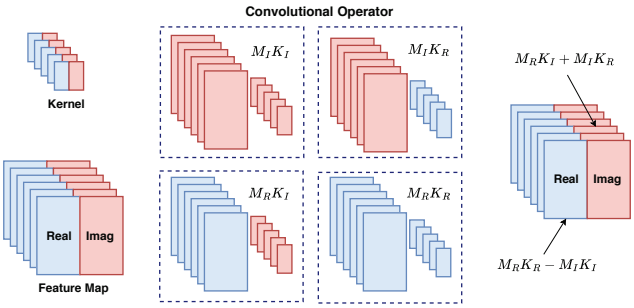

Figure 2. *Illustration of the complex convolution operator.*

3.3.2 Activation Unit

We employ Complex PReLU (CPReLU) as the complex activation function, which applies separate PReLUs to both the real and imaginary parts of a neuron, i.e.

$$\mathrm{CPReLU}(z) = \mathrm{PReLU}(z_R) + i\,\mathrm{PReLU}(z_I). \quad (22)$$

CPReLU satisfies the Cauchy-Riemann equations when both the real and imaginary parts are simultaneously either strictly positive or strictly negative.

3.3.3 Complex Differentiation and Chain Rules

When training neural networks, the backpropagation algorithm requires the calculation of gradients to update the weight parameters. However, the incorporation of complex values poses challenges for computing gradients of activation functions and loss functions during the backpropagation process. Suppose L is a real-valued loss function and z is a complex variable, where $z = x + iy$ and $x, y \in \mathbb{R}$. In this case, we have the following equations:

$$\begin{aligned}\nabla_L(z) &= \frac{\partial L}{\partial z} = \frac{\partial L}{\partial x} + i\frac{\partial L}{\partial y} \\ &= \frac{\partial L}{\partial \Re(z)} + i\frac{\partial L}{\partial \Im(z)} \\ &= \Re(\nabla_L(z)) + i\Im(\nabla_L(z)).\end{aligned} \quad (23)$$

Then, given another complex variable $t = r + is$ where z could be expressed in terms of t and r, $s \in \mathbb{R}$, we would have the complex chain rules

$$\begin{aligned}\nabla_L(t) &= \frac{\partial L}{\partial t} = \frac{\partial L}{\partial r} + i\frac{\partial L}{\partial s} \\ &= \frac{\partial L}{\partial x}\frac{\partial x}{\partial r} + \frac{\partial L}{\partial y}\frac{\partial y}{\partial r} + i\left(\frac{\partial L}{\partial x}\frac{\partial x}{\partial s} + \frac{\partial L}{\partial y}\frac{\partial y}{\partial s}\right) \\ &= \Re(\nabla_L(z))\left(\frac{\partial x}{\partial r} + i\frac{\partial x}{\partial s}\right) \\ &\quad + \Im(\nabla_L(z))\left(\frac{\partial y}{\partial r} + i\frac{\partial y}{\partial s}\right),\end{aligned} \quad (24)$$

as described in the literature [37].

3.4 RMCPNet for Downlink Transmission

In Figure 3, we present the overall architecture of RMCPNet. The network comprises four stacked layers: the input layer, the feature extraction layer stack, the feature fusion layer stack, and the output layer.

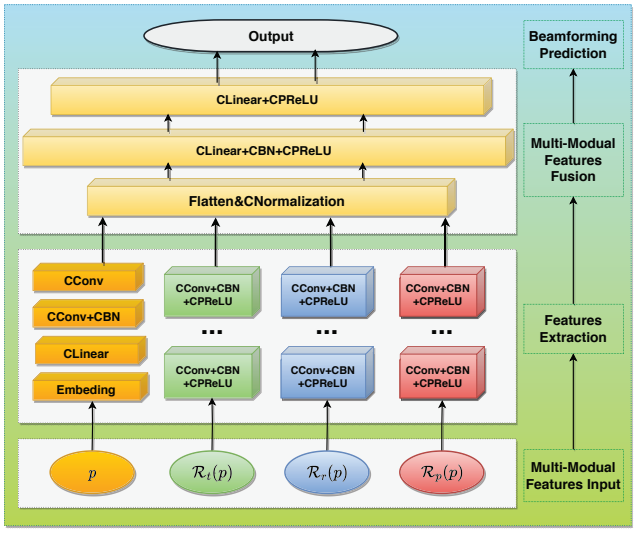

Figure 3. *The framework of RMCPNet.*

Considering the heterogeneity of different infor-

mation, we partition the information $\mathcal{S}(p)$ into four parallel subnetworks to input different position information and statistical information to the network, which achieves the feature extraction of heterogeneous information. For the position encoding subnetwork, we first convert the input two-dimensional position p into a complex number, and then map it to a higher-dimensional feature through a fully connected layer. The high-dimensional feature then undergoes a convolution layer, complex batch normalization, and two successive CConv layers to obtain the two-dimensional encoding of p. The transmission correlation matrix $\mathcal{R}_t(p)$, the reception correlation matrix $\mathcal{R}_r(p)$, and the channel fading matrix $\mathcal{R}_p(p)$ are processed by three successive CConv, CBN, and CPReLU layers, respectively, to obtain the channel transmission coherence encoding, reception coherence encoding and channel fading encoding. In the feature fusion layer, we use Flatten and CBN to concatenate and fuse the features obtained by the four subnetworks. After multi-modal information fusion, we use CLinear CBN and CPReLU to process the fused features. The network finally produces the precoding output $f_\theta(p, \mathcal{S}(p))$ through CPReLU.

In this paper, our objective is to maximize the spectral efficiency, which is equivalent to minimizing the negative spectral efficiency. Since we encounter difficulty obtaining the optimal precoding $\mathbf{w}$ by the Monte Carlo method, we can acquire the overall spectral efficiency when applying the precoding $\mathbf{w}_\theta(p)$ by equation (17). In the following, we denote a sample as

$$x = \{p, \mathcal{S}(p), \mathbf{H}\}. \tag{25}$$

Then, a batch of samples can be denoted as

$$\mathcal{X}_b \triangleq \{p_i, \mathcal{S}(p_i), \mathbf{H}_i | i \in 1, \ldots B_s\}, \tag{26}$$

where B_s is batch size. Therefore, the loss function can be calculated as

$$\mathcal{L}(p, H) = -\log_2 \det\left(\mathrm{I} + \rho \mathbf{H} f_\theta(p, \mathcal{S}(p)) f_\theta(p, \mathcal{S}(p))^{\mathrm{H}} \mathbf{H}^{\mathrm{H}}\right). \tag{27}$$

Algorithm 1. *RMCPNet training.*

Input: The dataset $\mathcal{D}$, model $f_\theta(\cdot)$, learning rate γ, batch size B_s, maximum iteration $I_{\max}$, terminate parameters N_{ter}, N_{lr}

Output: The trained model $f_\theta(\cdot)$

Initialize the RMCPNet model $f_\theta(\cdot)$ with $\theta \sim \mathcal{CN}(0, 0.01)$
partition $\mathcal{D}$ according to batch size B_s
epoch counter $i \leftarrow 0$
convergence label $\mathcal{C} =$ False
while $i \leq I_{\max}$ or $\mathcal{C}$ **do**
  for $b = 0, .., B-1$ **do**
    sample a batch $\mathcal{X}_b$ from $\mathcal{D}$
    compute loss $\mathcal{L}(\mathcal{X}_b)$
    compute the stochastic gradient of θ according to $\mathcal{L}(\mathcal{X}_b)$
    update model parameters f_θ with corresponding gradients and learning rate γ
    if L converges **then**
      $\mathcal{C} =$ True
      break
    end if
  end for
  $i = i + 1$
  update the learning rate γ
end while

When a batch of training data $\mathcal{X}_b$ is fed into the RMCPNet, we can obtain the average throughput loss $\mathcal{L}(\mathcal{X}_b)$ at this point. When training the network, the proposed training algorithm 1 is goal-oriented and directly trains the network, which updates the network parameters in the direction of maximizing $\mathcal{L}(\mathcal{X}_b)$. In this algorithm, we constrain the maximum epoch $I_{\max}$, and add an algorithm convergence condition to terminate the training early (whether the $\mathcal{L}(\mathcal{X}_b)$ obtained by successive N_{ter} epochs decreases). The learning rate γ is executed by exponential decay $\gamma = 0.9 * \gamma$ by detecting whether the $\mathcal{L}(\mathcal{X})$ obtained by successive N_{lr} epochs decreases.

IV. SIMULATION RESULTS

In this section, we explain the detailed simulation setup and show the comparison with several benchmark precoding methods.

4.1 Simulation Scenario and Data Collection

As illustrated in Figure 4, we consider the simulation scenario based on the DeepMIMO outdoor dynamic

scenario 'O2 Dynamic' [45] to study the performance of our proposed method. The major simulation hyperparameters are summarized in Table 1. There are two DBSs located in the area, and users are distributed in the green rectangular area $\mathcal{P}$ in which we sample up to 100,000 candidate positions to construct the radio map.

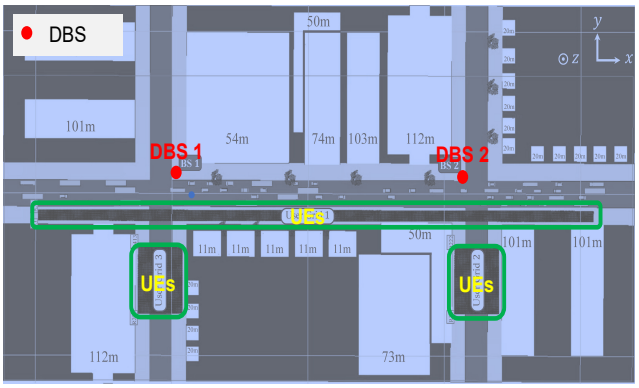

Figure 4. *The simulation scenario.*

Table 1. *Simulation hyperparameters.*

Parameters	Values
Simulation scenario	O2 Dynamic (Outdoor 2)
DBS number	2
Candidate positions	100000
Simulation slots	total 800, 600 for train, 200 for test
Channel model	Ray tracing
Center frequency	3.5 GHz
Multipath	10
Bandwidth	100MHz
DBS antenna	8×2 isotropic antenna array
User antenna	2×1 isotropic antenna array
OFDM	Number of FFT 256, Sub-carrier 30 KHz

We simulate 800 time slots to collect channel data. Specifically, the first 600 slots are used to generate the radio map $\mathcal{S}(p), p \in \mathcal{P}$ and train the RMCPNet $f_\theta\left(p, \mathcal{S}(p)\right)$, while the remaining 200 slots serve to verify the effectiveness of the proposed method. For each position $p \in \mathcal{P}$, we collect corresponding channels $\mathbf{H}$, and compute the radio statistical feature $\mathcal{S}(p)$, which constitutes a training sample $x_i = \{p, \mathcal{S}(p), \mathbf{H}\}$. Then, we can build the radio map $\mathcal{S}$ and acquire the dataset.

In this paper, we employ four benchmark methods to verify the efficacy of our proposed algorithm.

- No Precoding (NoP). No precoding is applied, and all antennas transmit simultaneously.
- Statistical Codebook (SCB). A codebook is used to select precoding. The precoding that has been used most frequently in the training slots at position p is adopted as the precoding for the user at that position for the test.
- Neural Networks (NN). We train real-valued neural networks with the same structure as complex neural networks to perform precoding among multiple antennas.
- Singular value decomposition (SVD). We calculate the precoding with SVD, which is the theoretically optimal method.

In Table 2, we describe the detailed structure of the RMCPNet. Next, we will simulate and validate the performance of the proposed algorithm from different perspectives.

Table 2. *RMCPNet structure description.*

Subnetwork	Structure
position embedding	128 units; 64 clinear; 16 2*1 CConv filters;
transmission embedding	16 3*3 CConv; 32 3*3 CConv; 16 2*2 CConv
reception embedding	16 2*2 CConv; 16 1*2 CConv; 8 2*1 CConv
power embedding	16 2*3 CConv; 16 2*3 CConv; 8 1*2 CConv
feature fusion	256 units; 128 units; 16 units

4.2 Channel Distribution of Angular Domain

Calculating the power azimuth spectrum (PAS) of the channel, we observed a strong correlation between the user's location/angle and the direction of maximum spectral energy density. Figure 5 delineates the PAS for precoding utilizing both a random sample and RMCPNet. We observe that the precoding obtained by RMCPNet can point more precisely to the angle and energy peaks of the channel, resulting in a higher received channel power as compared to the SCB method. This enhancement can be ascribed to the superior accuracy in beamforming directions afforded by our methodology. Moreover, since RMCPNet outputs the precoding vector, it can generate multiple beam directions in the spatial domain to accommodate the energy distribution of the channel small-scale fading in different directions. Consequently, our proposed strategy demonstrates superior performance and robustness in the face of channel variations.

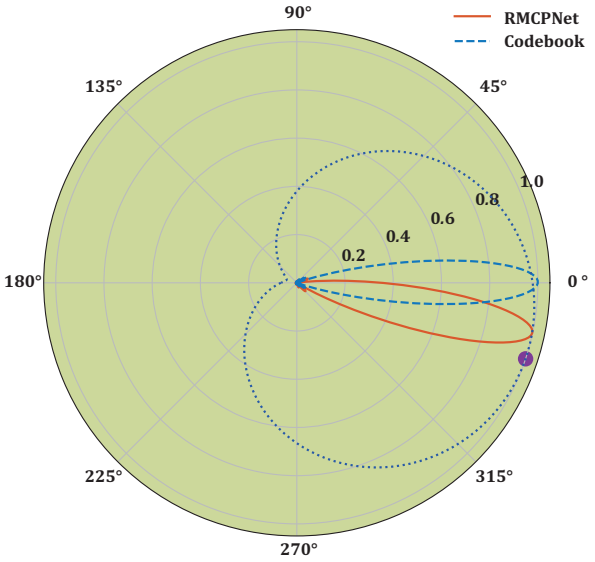

Figure 5. *The PAS for a sample of channel, RMCPNet precoding, and SCB precoding.*

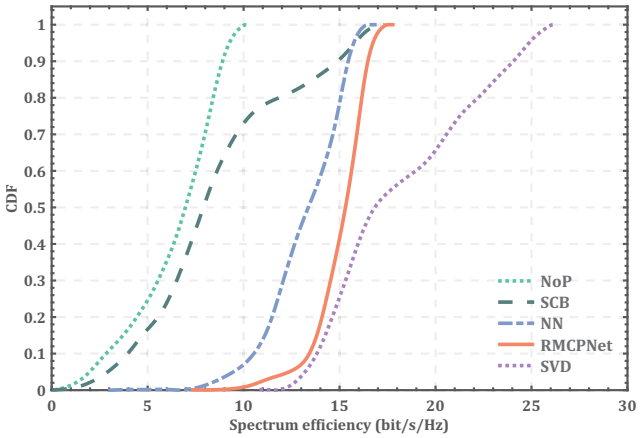

Figure 6. *The CDF of the average spectral efficiency for different algorithms.*

4.3 Spectral Efficiency

Figure 6 shows that the proposed RMCPNet method significantly outperforms the SCB and NN methods. Specifically, RMCPNet has very few users with spectral efficiency below 7 bit/Hz/s, while many users of the SCB method have spectral efficiency below 5 bit/Hz/s. Moreover, we find that the SCB method, which obtains the optimal precoding based on historical statistics, is challenging to work in the complex time-varying electromagnetic environment with multipath. In addition, compared to the NN method, RMCPNet can effectively reduce the probability of choosing suboptimal precoding. However, the major drawback of RMCPNet is that it cannot achieve a higher spectral efficiency level (above 15bit/s/Hz) compared with the optimal precoding scheme based on SVD. This is because the current RMCPNet does not introduce a multi-stream mechanism that can achieve spatial multiplexing.

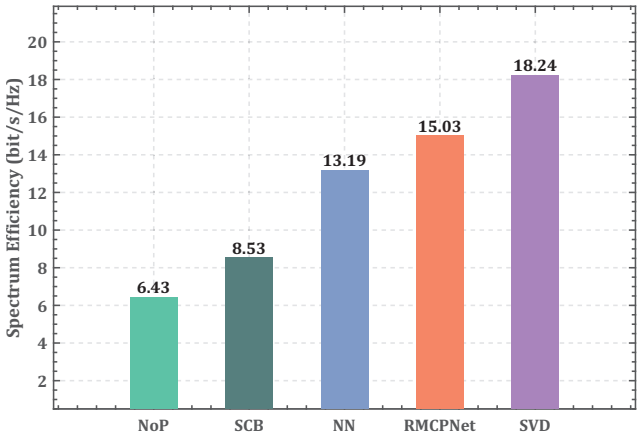

Figure 7. *The average spectral efficiency of different algorithms.*

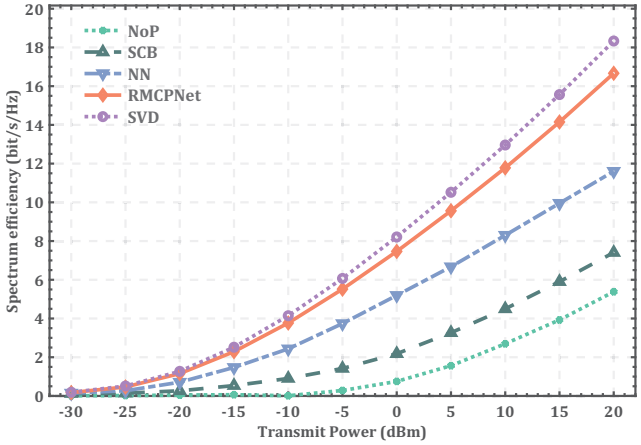

Figure 8. *The average spectral efficiency of different algorithms varies with the transmission power.*

Figure 7 compares the average spectral efficiency achieved by different algorithms. The proposed scheme is far superior to the statistical precoding method, boasting a performance enhancement of 76%. Compared with the NN approach, we still have a 16% performance improvement, which indicates that our network architecture design is more reliable. Compared with the optimal precoding based on SVD, RMCPNet can still achieve 82.4% of the optimal performance. This discrepancy presents an opportunity for future refinement, specifically through the adoption of

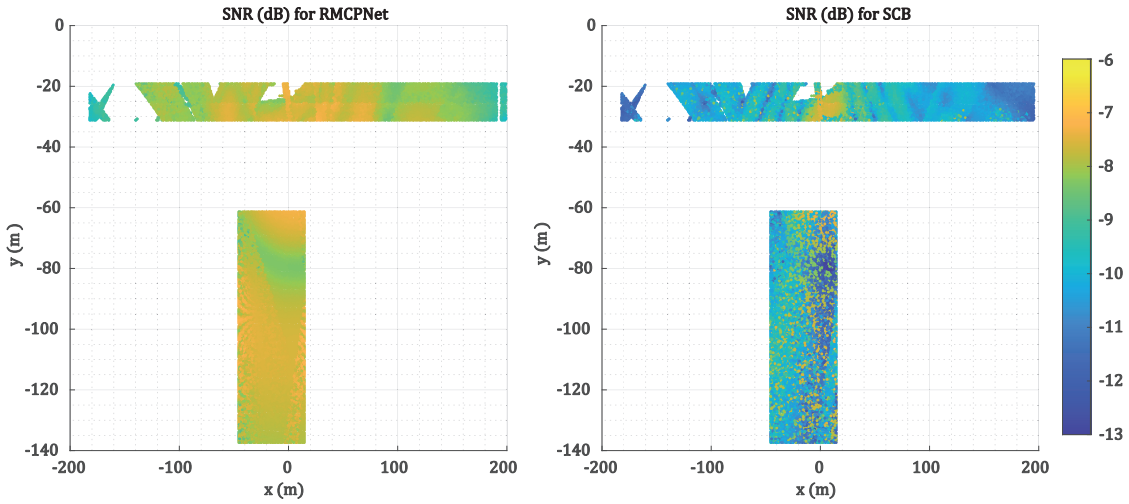

Figure 9. *SNR at different positions for RMCPNet and SCB, respectively. Note that the positions are left blank if there is no data available.*

a multi-stream technique.

In Figure 8, the transmission power of the base station is adjusted from -30dBm to 20dBm. It is observed that RMCPNet still achieves the best transmission performance compared to other single-stream transmission schemes, which demonstrates that our proposed algorithm is robust and can achieve good performance for different transmission powers.

According to the phenomena illustrated in Figure 6 and Figure 7, insights reveals that the observed performance enhancement stems chiefly from three factors: the radio map's adept characterization of the channel's statistical properties, the proposed multi-modal information fusion architecture's enhanced capability to distill the channel's intrinsic properties, and the complex neural processing unit's superior efficiency in handling complex channel values.

4.4 SNR at Different Positions

Figure 9 compares the signal-to-noise ratio (SNR) achieved by RMCPNet and the SCB method across various locations. Our method outperforms the SCB scheme, i.e., demonstrating superior signal coverage. Notably, the statistical codebook scheme generates more distinct beams in proximity to the base station, where SNR levels are elevated. Conversely, in regions distant from the base station, characterized by diminished SNR, there is a noticeable variability in the positions with high and low SNR within these areas. This variability may stem from the augmented unpredictability of channel energy distribution under low SNR conditions, leading to erratic codebook selection and suboptimal performance. In comparison, approach consistently maintains elevated SNR levels across the entire spatial domain, showcasing its robustness and effectiveness.

V. CONCLUSION

In this paper, we have proposed a transmission mechanism for downlink transmission in FD-RAN without relying on physical layer channel feedback. Furthermore, We have designed a complex-valued precoding network called RMCPNet based on the radio map. To leverage multimodal input information, including user location, channel transmit/recieve correlation matrix, and channel energy matrix, in the RMCPNet, we have further designed several different subnets for multimodal feature extraction. Then, the multimodal encoded features are fused at the feature fusion layer. Considering the computational complexity of obtaining optimal precoding, we have also proposed a specific network training algorithm with negative spectral efficiency as the loss function. The simulation results of RMCPNet on the public DeepMIMO dataset demonstrate that the proposed RMCPNet delivers significantly improved performance compared to traditional neural networks and the statistical precoding method.

In our future work, we plan to further study the impact of feedback delay on wireless transmission

and consider precoding in mobile scenarios with the help of predicting user location in real time. We will also implement the feedback-free beamforming method based on the predicted user position and channel statistical information on USRP hardware to verify the feasibility of the proposed scheme in a realistic environment. Furthermore, we will extend the current method to support multi-stream transmission. Additionally, we will study cooperative precoding of multiple base stations.

ACKNOWLEDGEMENT

This work was supported in part by the National Natural Science Foundation Original Exploration Project of China under Grant 62250004, the National Natural Science Foundation of China under Grant 62271244, the Natural Science Fund for Distinguished Young Scholars of Jiangsu Province under Grant BK20220067, and the Natural Sciences and Engineering Research Council of Canada (NSERC).

References

[1] G. Liu, Y. Huang, *et al.*, "Vision, requirements and network architecture of 6g mobile network beyond 2030," *China Communications*, 2020, vol. 17, no. 9, pp. 92–104.

[2] Q. Yu, H. Zhou, *et al.*, "A fully-decoupled ran architecture for 6g inspired by neurotransmission," *Journal of Communications and Information Networks*, 2019, vol. 4, no. 4, pp. 15–23.

[3] S. Dang, O. Amin, *et al.*, "What should 6g be?" *Nature Electronics*, 2020, vol. 3, no. 1, pp. 20–29.

[4] X. Wang, J. Mei, *et al.*, "Realizing 6g: The operational goals, enabling technologies of future networks, and value-oriented intelligent multi-dimensional multiple access," *IEEE Network*, 2023, vol. 37, no. 1, pp. 10–17.

[5] B. Qian, T. Ma, *et al.*, "Enabling fully-decoupled radio access with elastic resource allocation," *IEEE Transactions on Cognitive Communications and Networking*, 2023.

[6] Y. Xu, H. Zhou, *et al.*, "Leveraging multiagent learning for automated vehicles scheduling at nonsignalized intersections," *IEEE Internet of Things Journal*, 2021, vol. 8, no. 14, pp. 11 427–11 439.

[7] H. Cui, J. Zhang, *et al.*, "Space-air-ground integrated network (sagin) for 6g: Requirements, architecture and challenges," *China Communications*, 2022, vol. 19, no. 2, pp. 90–108.

[8] D. Tse and P. Viswanath, *Fundamentals of Wireless Communication*. Cambridge University Press, 2005.

[9] C. Wen, W. Shih, *et al.*, "Deep learning for massive mimo csi feedback," *IEEE Wireless Communications Letters*, 2018, vol. 7, no. 5, pp. 748–751.

[10] G. Zhou, C. Pan, *et al.*, "A framework of robust transmission design for irs-aided miso communications with imperfect cascaded channels," *IEEE Transactions on Signal Processing*, 2020, vol. 68, pp. 5092–5106.

[11] K. Yu, Q. Yu, *et al.*, "Fully-decoupled radio access networks: A flexible downlink multi-connectivity and dynamic resource cooperation framework," *IEEE Transactions on Wireless Communications*, 2023, vol. 22, no. 6, pp. 4202–4214.

[12] D. Deng, C. Wang, *et al.*, "Joint flexible duplexing and power allocation with deep reinforcement learning in cell-free massive mimo system," *China Communications*, 2023, vol. 20, no. 4, pp. 73–85.

[13] C. Luo, J. Ji, *et al.*, "Channel state information prediction for 5g wireless communications: A deep learning approach," *IEEE Transactions on Network Science and Engineering*, 2018, vol. 7, no. 1, pp. 227–236.

[14] L. Xiao, S. Li, *et al.*, "Error probability analysis for ultra-massive mimo system and near-optimal signal detection," *China Communications*, 2023, vol. 20, no. 5, pp. 1–19.

[15] J. Zhao, Q. Yu, *et al.*, "Fully-decoupled radio access networks: A resilient uplink base stations cooperative reception framework," *IEEE Transactions on Wireless Communications*, 2023.

[16] J. Shen, J. Zhang, *et al.*, "Compressed csi acquisition in fdd massive mimo: How much training is needed?" *IEEE Transactions on Wireless Communications*, 2016, vol. 15, no. 6, pp. 4145–4156.

[17] J. Guo, C. Wen, *et al.*, "Convolutional neural network-based multiple-rate compressive sensing for massive mimo csi feedback: Design, simulation, and analysis," *IEEE Transactions on Wireless Communications*, 2020, vol. 19, no. 4, pp. 2827–2840.

[18] M. B. Mashhadi, Q. Yang, *et al.*, "Distributed deep convolutional compression for massive mimo csi feedback," *IEEE Transactions on Wireless Communications*, 2020, vol. 20, no. 4, pp. 2621–2633.

[19] Z. Yin, W. Xu, *et al.*, "Deep compression for massive mimo: A self-information model-driven neural network," *IEEE Transactions on Wireless Communications*, 2022, vol. 21, no. 10, pp. 8872–8886.

[20] X. Song, J. Wang, *et al.*, "Saldr: Joint self-attention learning and dense refine for massive mimo csi feedback with multiple compression ratio," *IEEE Wireless Communications Letters*, 2021, vol. 10, no. 9, pp. 1899–1903.

[21] J. Wang, G. Gui, *et al.*, "Compressive sampledcsi feedback method based on deep learning for fdd massive mimo systems," *IEEE Transactions on Communications*, 2021, vol. 69, no. 9, pp. 5873–5885.

[22] X. Gao, B. Jiang, *et al.*, "Statistical eigenmode transmission over jointly correlated mimo channels," *IEEE Transactions on Information Theory*, 2009, vol. 55, no. 8, pp. 3735–3750.

[23] E. Björnson, M. Bengtsson, *et al.*, "Optimal multiuser transmit beamforming: A difficult problem with a simple solution structure," *IEEE Signal Processing Magazine*, 2014, vol. 31, no. 4, pp. 142–148.

[24] J. Kim, H. Lee, *et al.*, "Learning robust beamforming for miso downlink systems," *IEEE Communications Letters*, 2021, vol. 25, no. 6, pp. 1916–1920.

[25] W. Wang, X. Chen, *et al.*, "Artificial noise assisted secure

massive mimo transmission exploiting statistical csi," *IEEE Communications Letters*, 2019, vol. 23, no. 12, pp. 2386–2389.
[26] J. Shi, W. Wang, *et al.*, "Deep learning-based robust precoding for massive mimo," *IEEE Transactions on Communications*, 2021, vol. 69, no. 11, pp. 7429–7443.
[27] W. Peng, W. Li, *et al.*, "Downlink channel prediction for time-varying fdd massive mimo systems," *IEEE Journal of Selected Topics in Signal Processing*, 2019, vol. 13, no. 5, pp. 1090–1102.
[28] C. Luo, J. Ji, *et al.*, "Channel state information prediction for 5g wireless communications: A deep learning approach," *IEEE Transactions on Network Science and Engineering*, 2020, vol. 7, no. 1, pp. 227–236.
[29] M. Alrabeiah and A. Alkhateeb, "Deep learning for mmwave beam and blockage prediction using sub-6 ghz channels," *IEEE Transactions on Communications*, 2020, vol. 68, no. 9, pp. 5504–5518.
[30] C. Liu, W. Yuan, *et al.*, "Location-aware predictive beamforming for uav communications: A deep learning approach," *IEEE Wireless Communications Letters*, 2020, vol. 10, no. 3, pp. 668–672.
[31] M. Koivisto, A. Hakkarainen, *et al.*, "High-efficiency device positioning and location-aware communications in dense 5g networks," *IEEE Communications Magazine*, 2017, vol. 55, no. 8, pp. 188–195.
[32] P. Kela, M. Costa, *et al.*, "Location based beamforming in 5g ultra-dense networks," in *2016 IEEE 84th Vehicular Technology Conference (VTC-Fall)*, 2016, pp. 1–7.
[33] W. Miao, C. Luo, *et al.*, "Location-based robust beamforming design for cellular-enabled uav communications," *IEEE Internet of Things Journal*, 2020, vol. 8, no. 12, pp. 9934–9944.
[34] A. Alkhateeb, S. Alex, *et al.*, "Deep learning coordinated beamforming for highly-mobile millimeter wave systems," *IEEE Access*, 2018, vol. 6, pp. 37 328–37 348.
[35] B. Zhou, A. Liu, *et al.*, "Successive localization and beamforming in 5g mmwave mimo communication systems," *IEEE Transactions on Signal Processing*, 2019, vol. 67, no. 6, pp. 1620–1635.
[36] C. Liu, W. Yuan, *et al.*, "Learning-based predictive beamforming for integrated sensing and communication in vehicular networks," *IEEE Journal on Selected Areas in Communications*, 2022, vol. 40, no. 8, pp. 2317–2334.
[37] C. Trabelsi, O. Bilaniuk, *et al.*, "Deep complex networks," in *6th International Conference on Learning Representations, ICLR 2018, Vancouver, BC, Canada, April 30 - May 3, 2018, Conference Track Proceedings*. OpenReview.net, 2018.
[38] T. Fang and J. Sun, "Stability of complex-valued recurrent neural networks with time-delays," *IEEE Transactions on Neural Networks and Learning Systems*, 2014, vol. 25, no. 9, pp. 1709–1713.
[39] C. Zhang, H. Lu, *et al.*, "Imreconet: Learn to detect in index modulation aided mimo systems with complex valued neural networks," *IEEE Transactions on Vehicular Technology*, 2023, vol. 72, no. 2, pp. 1791–1805.
[40] Y. Yang, F. Gao, *et al.*, "Deep learning-based downlink channel prediction for fdd massive mimo system," *IEEE Communications Letters*, 2019, vol. 23, no. 11, pp. 1994–1998.
[41] Y. Tu, Y. Lin, *et al.*, "Complex-valued networks for automatic modulation classification," *IEEE Transactions on Vehicular Technology*, 2020, vol. 69, no. 9, pp. 10 085–10 089.
[42] Z. Zhao, M. C. Vuran, *et al.*, "Deep-waveform: A learned ofdm receiver based on deep complex-valued convolutional networks," *IEEE Journal on Selected Areas in Communications*, 2021, vol. 39, no. 8, pp. 2407–2420.
[43] Y. Wang, G. Gui, *et al.*, "An efficient specific emitter identification method based on complex-valued neural networks and network compression," *IEEE Journal on Selected Areas in Communications*, 2021, vol. 39, no. 8, pp. 2305–2317.
[44] S. Ji and M. Li, "Clnet: Complex input lightweight neural network designed for massive mimo csi feedback," *IEEE Wireless Communications Letters*, 2021, vol. 10, no. 10, pp. 2318–2322.
[45] A. Alkhateeb, "Deepmimo: A generic deep learning dataset for millimeter wave and massive mimo applications," in *Proc. of Information Theory and Applications Workshop (ITA)*, San Diego, CA, 2019, pp. 1–8.

Biographies

Zhao Jiwei received the M.S. degree in information and communication system from Xidian University, Xi'an, China, in 2018. He is currently working toward the Ph.D degree with the School of Electronic Science and Engineering, Nanjing University, Nanjing, China. He won the first prize in the 2016 CCF China Big Data and Cloud Computing Intelligence Contest. His research interests include fully-decoupled RAN architecture, coordinated multi-point, and machine learning applications for wireless communication.

Chen Jiacheng received the Ph.D degree in information and communications engineering from Shanghai Jiao Tong University, Shanghai, China, in 2018. From December 2015 to December 2016, he was a Visiting Scholar with BBCR group, University of Waterloo, Waterloo, ON, Canada. He is currently an Assistant Researcher with Peng Cheng Laboratory, Shenzhen, China. His research interests include future network design, 5G/6G network, and resource management. He was the recipient of the Journal of Communications and Information Networks (JCIN) Best Paper Award in 2016, and the Chinese Institute of Electronics (CIE) Best Paper Award in Electronic and Information in 2020. He was the Guest Editor for the *IEEE Internet of Things Journal* and *Journal of Communications and Information Networks*, and the Workshop Co-Chair for the IEEE/CIC ICCC'21.

Sun Zeyu received B.S. degree in electronic science and technology from Xidian University, Xi'an, China, in 2022. He is currently pursuing the Ph.D degree with Nanjing University, Nanjing, China. His research interests include B5G/6G networks, high speed train communication, blockchain and machine learning for wireless communications.

Shi Yuhang is currently pursuing the B.S. degree with the School of Electronic Engineering, Xidian University, Xi'an, China. His current research interests include MIMO wireless communication PHY algorithms, full-decoupling radio access network and artificial intelligence.

Zhou Haibo received the Ph.D degree in information and communication engineering from Shanghai Jiao Tong University, Shanghai, China, in 2014. From 2014 to 2017, he was a Postdoctoral Fellow with the Broadband Communications Research Group, Department of Electrical and Computer Engineering, University of Waterloo. He is currently a Full Professor with the School of Electronic Science and Engineering, Nanjing University, Nanjing, China. He was a recipient of the 2019 IEEE ComSoc Asia-Pacific Outstanding Young Researcher Award. He served as Track/Symposium Co-Chair for IEEE/CIC ICCC 2019, IEEE VTC-Fall 2020, IEEE VTC-Fall 2021, and IEEE GLOBECOM 2022. He is currently an Associate Editor of the *IEEE Transactions on Wireless Communications, IEEE Internet of Things Journal, IEEE Network Magazine*, and *IEEE Wireless Communications Letter*. His research interests include resource management and protocol design in B5G/6G networks, vehicular ad hoc networks, and space-air-ground integrated networks.

Xuemin (Sherman) Shen (M'97-SM'02-F'09) received the Ph.D degree in electrical engineering from Rutgers University, New Brunswick, NJ, USA, in 1990. He is a University Professor with the Department of Electrical and Computer Engineering, University of Waterloo, Canada. His research focuses on network resource management, wireless network security, Internet of Things, 5G and beyond, and vehicular networks. Dr. Shen is a registered Professional Engineer of Ontario, Canada, an Engineering Institute of Canada Fellow, a Canadian Academy of Engineering Fellow, a Royal Society of Canada Fellow, a Chinese Academy of Engineering Foreign Member, and a Distinguished Lecturer of the IEEE Vehicular Technology Society and Communications Society.